Title	A Monte Carlo study of the intrinsic viscosity of semiflexible ring polymers
Author(s)	Ono, Yuki; Ida, Daichi
Citation	Polymer Journal (2015), 47(7): 487-492
Issue Date	2015-04-15
URL	http://hdl.handle.net/2433/201541
Right	© 2015 The Society of Polymer Science, Japan
Type	Journal Article
Textversion	author

A Monte Carlo study of the intrinsic viscosity of semiflexible ring polymers

Yuki Ono and Daichi Ida

Department of Polymer Chemistry, Kyoto University, Kyoto, Japan

Correspondence: Dr. D. Ida, Department of Polymer Chemistry, Kyoto University, Katsura, Kyoto 615-8510, Japan.

E-mail: ida@molsci.polym.kyoto-u.ac.jp

ABSTRACT: A Monte Carlo study is made of the intrinsic viscosity $[\eta]$ of semiflexible ring polymers by the use of a discrete version of the Kratky–Porod (KP) wormlike ring without excluded volume. The values of $[\eta]$ are evaluated in the Kirkwood–Riseman approximation. The ratio of $[\eta]$ of the rings of the trivial knot to that of the rings without the topological constraint is found to become a function only of the reduced contour length λL, where λ^{-1} is the stiffness parameter of the KP chain and L is the total contour length. It is then shown that the ratio is almost equal to unity for $\lambda L \lesssim 10$ and increases monotonically with increasing λL for $\lambda L \gtrsim 10$.

KEYWORDS: Monte Carlo simulation; intrinsic viscosity; ring polymer; semiflexible polymer; wormlike chain model

INTRODUCTION

We have recently made Monte Carlo (MC) studies[1–3] of effects of chain stiffness on dilute solution properties of unperturbed ring polymers by the use of a discrete version[4] of the Kratky–Porod (KP) wormlike chain model[5,6] without excluded volume. The behavior of the second virial coefficient A_2 in the unperturbed (Θ) state, which is proportional to the effective intermolecular excluded volume arising only from the topological interaction,[1] and that of the scattering function $P(k)$ with k the magnitude of the scattering vector[2] were examined as functions of the reduced contour length λL, where λ^{-1} is the stiffness parameter of the KP ring and L is the total contour length. Furthermore, effects of the intramolecular topological constraint, which works to preserve a given knot type of a single ring polymer, on A_2 and $P(k)$ and also on the mean-square radius of gyration $\langle S^2 \rangle$ [1] were examined by comparing the MC results for the following two kinds of the equilibrium ensembles of configurations of the KP rings: one is the ensemble composed of configurations only of the trivial knot, called the *trivial-knot ensemble*, and the other is that composed of configurations of all kinds of knot with the Boltzmann weight of the configurational potential energy, called the *mixed ensemble*. Hereafter, the subscripts "t.k." and "mix" are used to denote the values for the trivial-knot and mixed ensembles, respectively. It was shown that the difference between the two kinds of ensembles becomes large with increasing λL for large λL, while both the ensembles are, of course, identical with each other in the rigid-ring limit $\lambda L \to 0$. Specifically, the ratio $\langle S^2 \rangle_{\rm t.k.}/\langle S^2 \rangle_{\rm mix}$ (both the values being for the same λ^{-1} and L) was found to be almost equal to unity for $\lambda L \lesssim 10$ and increase monotonically with increasing λL for $\lambda L \gtrsim 10$. However, the range of $\lambda L \leq 10^3$ so investigated was still far from the random-coil limit of $\lambda L \to \infty$. We note that in this limit there holds the asymptotic relation $\langle S^2 \rangle_{\rm t.k.}/\langle S^2 \rangle_{\rm mix} \propto (\lambda L)^{0.2}$ derived from the relations $\langle S^2 \rangle_{\rm mix} \propto \lambda L$ [7–9] and $\langle S^2 \rangle_{\rm t.k.} \propto (\lambda L)^{2\nu}$ with $\nu \simeq 0.6$.[10,11]

As a continuation of the previous studies, the present study adresses the intrinsic viscosity $[\eta]$ of semiflexible ring polymers. The quantity $[\eta]$ works as a measure of average chain dimension of polymers in solution and is strongly affected by the primary structure of polymers as well as by the chain stiffness, since $[\eta]$ is related to the effective hydrodynamic volume of

polymers in solution (in shear flow) by the Einstein formula for $[\eta]$ of rigid spheres.[9] For a deeper understanding of the effects of the topological constraint and also chain stiffness on the conformational properties of ring polymers, it is necessary to clarify the behavior of $[\eta]_{\rm t.k.}/[\eta]_{\rm mix}$ (both the values being for the same λ^{-1} and L) as a function of λL in the range of the crossover from the rigid-ring limit to the random-coil one. We note that in the random-coil limit there holds the asymptotic relation $[\eta]_{\rm t.k.}/[\eta]_{\rm mix} \propto (\lambda L)^{3\nu-3/2}$ ($3\nu - 3/2 \simeq 0.3$) considering the fact that $[\eta]$ is proportional to $\langle S^2\rangle^{3/2}$ in this limit along with the asymptotic relations for $\langle S^2\rangle$ described above. Such a study may contribute to the progress in the fine characterization of novel ring polymer samples, for example, well-purified ring polystyrene[12] and cyclic amylose tris(alkylcarbamate)s.[13]

As in the cases of the previous studies,[1,2] we resort to the MC method for evaluating $[\eta]$ of the KP rings because of the formidable difficulty in analytical treatment of the topological constraint. We evaluate $[\eta]_{\rm mix}$ and $[\eta]_{\rm t.k.}$ of the KP rings for various values of λ^{-1} and L in the Kirkwood–Riseman (KR) approximation.[9,14] On the basis of the values of $[\eta]_{\rm mix}$ and $[\eta]_{\rm t.k.}$ so obtained, the behavior of $[\eta]_{\rm t.k.}/[\eta]_{\rm mix}$ is examined. Furthermore, the Flory–Fox factor[9,15] Φ defined from $[\eta]$ and $\langle S^2\rangle$ by

$$[\eta] = 6^{3/2}\Phi\frac{\langle S^2\rangle^{3/2}}{M} \tag{1}$$

with M the molecular weight is calculated both for the mixed and trivial-knot ensembles using with the MC values of $[\eta]$ along with those of $\langle S^2\rangle$ obtained in the previous study, and then, the behavior of $\Phi_{\rm mix}$, $\Phi_{\rm t.k.}$, and $\Phi_{\rm t.k.}/\Phi_{\rm mix}$ as functions of λL is also examined.

It is pertinent to note here the theoretical study of $[\eta]$ of the (continuous) KP ring by Fujii and Yamakawa.[16] They have already obtained an analytical expression for $[\eta]_{\rm mix}$ of the KP ring along with that of the rigid ring in the KR approximation by the use of the hydrodynamic cylinder model.[6] Their expression has been given as a function not only of λL but also λd with d the hydrodynamic diameter of the cylinder. Unfortunately, however, the expression is available only in a limited range of large λL. In anticipation of results, we note that the present MC study may cover the range of small λL, although only in part and numerically.

MODEL AND METHODS

Model and MC sampling

The MC model and method used in this study are the same as those in the previous study of A_2,[1] so that we here give a brief description. The (ideal) discrete KP ring[4] is composed of n (junction) points connected by n infinitely thin bonds of length l. Let $\mathbf{l}_i$ ($i = 1, 2, \cdots, n-1$) be the ith bond vector from the ith point to the $(i+1)$th. The nth bond vector $\mathbf{l}_n$ completes the ring, $\sum_{i=1}^{n} \mathbf{l}_i = \mathbf{0}$. The configuration of the ring may then be specified by the set $\{\mathbf{l}_n\} = [\mathbf{l}_1, \mathbf{l}_2, \cdots, \mathbf{l}_{n-1}(, \mathbf{l}_n)]$ apart from its position and orientation in an external Cartesian coordinate system, $\mathbf{l}_n$ being a dependent variable for the ring. Let θ_i ($i = 2, 3, \cdots, n$) be the angle between $\mathbf{l}_{i-1}$ and $\mathbf{l}_i$ and θ_1 between $\mathbf{l}_n$ and $\mathbf{l}_1$. The configurational potential energy U of the ring may be given by

$$U(\{\mathbf{l}_n\}) = \frac{\alpha}{2} \sum_{i=1}^{n} {\theta_i}^2 \,, \tag{2}$$

where α is the bending force constant. The stiffness parameter λ^{-1} of the chain may be given by

$$\lambda^{-1} = l \frac{1 + \langle \cos\theta \rangle}{1 - \langle \cos\theta \rangle} \,, \tag{3}$$

where $\langle \cos\theta \rangle$ is defined by

$$\langle \cos\theta \rangle = \int_0^\pi e^{-\alpha\theta^2/2k_\mathrm{B}T} \cos\theta \sin\theta \, d\theta \Big/ \int_0^\pi e^{-\alpha\theta^2/2k_\mathrm{B}T} \sin\theta \, d\theta \tag{4}$$

with k_B the Boltzmann constant and T the absolute temperature. The discrete KP ring so defined becomes identical with the continuous KP ring of total contour length L and of stiffness parameter λ^{-1} in the limit of $n \to \infty$ under the conditions of Equation (3) with Equation (4) and of $nl = L$.[4,17] Note that the MC model reduces to the freely jointed chain in the limit of $\alpha \to 0$. We adopt an n-sided regular polygon of side length l as the initial configuration and sequentially generate configurations without consideration of the topological constraint by the use of the Deutsch procedure[18] along with the Metropolis method of importance sampling,[19] its detail being described in the previous paper.[1]

An ensemble of configurations so obtained is a mixed ensemble. Following the procedure of Vologodskii *et al.*[20] to distinguish the trivial knot from the others by the use of the Alexander

polynomial,[21] we extract configurations with the trivial knot from not a few mixed ensembles and construct the trivial-knot ensemble.

All of the numerical work was done using a personal computer with an Intel Core i7-3770 CPU. A source program coded in C was compiled by the GNU C compiler version 4.8.4 with real variables of double precision. For the generation of pseudorandom numbers, the subroutine package MT19937 supplied by Matsumoto and Nishimura[22] was used instead of the subroutine RAND included in the standard C library.

Intrinsic viscosity

We consider the touched-bead KP ring model composed of n identical spherical beads of *hydrodynamic* diameter $d_\mathrm{b} = l$, whose centers are located at the n junctions of the discrete KP rings. If the model is immersed in a solvent having a simple shear flow field in the direction of the x axis in the external Cartesian coordinate system $(\mathbf{e}_x, \mathbf{e}_y, \mathbf{e}_z)$, $[\eta]$ (without consideration of a frictional force distribution on the surface of each bead) may be written in terms of the (total) frictional force ${\mathbf{F}_i}^T = (F_{ix}, F_{iy}, F_{iz})$ exerted by the ith bead ($i = 0, 1, 2, \cdots, n-1$) on the surrounding solvent and the position vector ${\mathbf{r}_i}^T = (r_{ix}, r_{iy}, r_{iz})$ of the center of ith bead, with the superscript T indicating the transpose, as follows,[9]

$$[\eta] = -\frac{N_\mathrm{A}}{2M\eta_0 g}\sum_{i=0}^{n-1}\langle F_{ix}r_{iy} + F_{iy}r_{ix}\rangle\,, \tag{5}$$

where N_A is the Avogadro constant, η_0 is the viscosity coefficient of the solvent, g is the velocity gradient of the flow field, and $\langle\cdots\rangle$ denotes the equilibrium ensemble average. The frictional force $\mathbf{F}_i$ satisfies the following simultaneous equations,

$$\mathbf{F}_i = \zeta(\mathbf{u}_i - \mathbf{v}_i^0) - \zeta\sum_{\substack{j=0\\ \neq i}}^{n-1}\mathbf{T}_{ij}\cdot\mathbf{F}_j\,, \tag{6}$$

where ζ is the friction coefficient of the bead given by the Stokes relation $\zeta = 3\pi\eta_0 d_\mathrm{b}$, $\mathbf{u}_i$ is the velocity of the ith bead, $\mathbf{v}_i^0$ is the unperturbed velocity of the solvent at the center of the ith bead, and $\mathbf{T}_{ij}$ is the Oseen tensor representing the hydrodynamic interaction between the ith and jth beads.

In the KR approximation,[9,14] the polymer chain in the simple shear flow field is assumed to move with the translational velocity equal to that of the flow field at the center of mass of

the chain and to rotate around its center of mass with the angular velocity $-\frac{1}{2}\mathbf{e}_z$. Under this assumption, the center of mass of the chain may be considered to be fixed at the origin of the external Cartesian coordinate system. Thus, $\mathbf{r}_i$ becomes identical with the vector distance $\mathbf{S}_i$ of the center of the $i$the bead from the center of mass of the chain and we may put

$$\mathbf{u}_i - \mathbf{v}_i^0 = \frac{1}{2} g(\mathbf{e}_x\mathbf{e}_y + \mathbf{e}_y\mathbf{e}_x) \cdot \mathbf{S}_i \,. \tag{7}$$

Further, $\mathbf{T}_{ij}$ is replaced by $\langle \mathbf{T}_{ij} \rangle$ given by

$$\langle \mathbf{T}_{ij} \rangle = \frac{1}{6\pi\eta_0} \langle R_{ij}^{-1} \rangle \mathbf{I} \,, \tag{8}$$

where R_{ij} is the distance between the centers of the ith and $j$the beads and $\mathbf{I}$ is the 3×3 unit tensor. This is the so-called preaveraging approximation for $\mathbf{T}_{ij}$.

In practice, the values of $[\eta]$ for each kind of the ensembles are evaluated as follows: First, $\langle R_{ij}^{-1} \rangle$ is calculated for each kind of the ensembles. Then, the simultaneous equations (6) with Equation (7) (and $\mathbf{r}_i = \mathbf{S}_i$) are solved by the use of $\langle \mathbf{T}_{ij} \rangle$ given by Equation (8) with $\langle R_{ij}^{-1} \rangle$ so obtained in place of $\mathbf{T}_{ij}$ for each sample configuration with randomizing its orientation with respect to the external system. Finally, $[\eta]$ is calculated from Equation (5).

RESULTS AND DISCUSSION

We carried out MC simulations for the (ideal) discrete KP touched-bead rings ($d_\mathrm{b} = l$) with n = 10, 20, 50, 100, and 200 and with $\alpha/k_\mathrm{B}T$ = 0, 0.3, 1, 3, 10, 30, 100; the $\alpha/k_\mathrm{B}T$ values correspond to λ^{-1}/l = 1, 2.575, 6.421, 20.36, 60.34, and 200.3, respectively, as calculated from Equation (3) with Equation (4). Extra MC simulations were carried out for the rings with $\alpha/k_\mathrm{B}T = 0$ (freely jointed chain) and for n = 500 and 1000. To keep the mean number of (real) configurational changes at every M_nom (nominal) steps nearly equal to n, we set $M_\mathrm{nom} = n$ for $\alpha/k_\mathrm{B}T = 0$, $M_\mathrm{nom} \simeq 2n$ for $\alpha/k_\mathrm{B}T = 0.3$ and 1, $M_\mathrm{nom} \simeq 5n$ for $\alpha/k_\mathrm{B}T = 3$ and 10, and $M_\mathrm{nom} \simeq 10n$ for $\alpha/k_\mathrm{B}T = 30$ and 100. Five mixed ensembles and five trivial-knot ones were then constructed for each case of $\alpha/k_\mathrm{B}T$ and n, each of which are constituted of 10^5 configurations except for $\alpha/k_\mathrm{B}T = 0$ and n = 1000. For that case, each ensemble was constituted of 10^4 configurations.

Table 1

The values of $M[\eta]_{\rm mix}/N_{\rm A}n^{3/2}l^3$ and their statistical errors, which are the mean and the standard deviation, respectively, of five independent MC runs for given values of $\alpha/k_{\rm B}T$ and n, are given in the second column of Table 1. In the fourth column are given the values of $M[\eta]_{\rm t.k.}/N_{\rm A}n^{3/2}l^3$ and their statistical errors evaluated in the same manner as above. (Recall that both of $[\eta]_{\rm mix}$ and $[\eta]_{\rm t.k.}$ have been evaluated for $d_{\rm b} = l$.) In the third and fifth columns are also given the corresponding values of $\langle S^2\rangle_{\rm mix}/nl^2$ and $\langle S^2\rangle_{\rm t.k.}/nl^2$, respectively, reproduced from Table 2 of ref 1.

Figure 1

Figure 1 shows double-logarithmic plots of $\lambda^{3/2}M[\eta]/N_{\rm A}L^{3/2}$ against λL. The open and closed circles represent the MC values of the mixed ($[\eta]_{\rm mix}$) and trivial-knot ensembles ($[\eta]_{\rm t.k.}$), respectively, for $\alpha/k_{\rm B}T = 0$ (pip up), 0.3 (pip right-up), 1 (pip right), 3 (pip right-down), 10 (pip down), 30 (pip left-down), and 100 (pip left). The dashed curves connect smoothly the MC values of $\lambda^{3/2}M[\eta]_{\rm mix}/N_{\rm A}L^{3/2}$ for each $\alpha/k_{\rm B}T$.

The quantity $\lambda^{3/2}M[\eta]_{\rm mix}/N_{\rm A}L^{3/2}$ increases monotonically with increasing λL for $\alpha/k_{\rm B}T \geq 1$, while for $\alpha/k_{\rm B}T \leq 0.3$ it decreases monotonically, in the range of λL investigated. In the cases of $\alpha/k_{\rm B}T \leq 1$, $\lambda^{3/2}M[\eta]_{\rm mix}/N_{\rm A}L^{3/2}$ seems to approach, although slowly, the random-coil limiting value[16,23,24] of 0.3078, as indicated by the solid horizontal line segment in Figure 1, with increasing λL. The MC values of $\lambda^{3/2}M[\eta]_{\rm mix}/N_{\rm A}L^{3/2}$ becomes larger with increasing $\lambda d_{\rm b}$ at constant λL, where $\lambda d_{\rm b}$ is the reduced hydrodynamic diameter and is equal to 1, 0.7102, 0.3883, 0.1557, 0.04912, 0.01657, and 0.004993 for $\alpha/k_{\rm B}T = 0$, 0.3, 1, 3, 10, 30, and 100, respectively.

In Figure 1, the solid curves represent the corresponding theoretical values of $[\eta]_{\rm mix}$ of the KP cylinder ring model of the hydrodynamic diameter d calculated from[16]

$$\frac{\lambda^{3/2}M[\eta]_{\rm mix}}{L^{3/2}} = \phi_\infty F(\lambda L, \lambda d)\,, \tag{9}$$

where $\phi_\infty = 1.854 \times 10^{23}$ mol^{-1} and

$$F(L,d) = \left[1 + \sum_{i=1}^{4} C_i(d) L^{-i/2}\right]^{-1} \tag{10}$$

with $C_i(d)$ given by

$$\begin{aligned}
C_1(d) &= 0.809231 - 40.8202d - 483.899d^2 - (2.53944 + 339.266d^2)\ln d \\
C_2(d) &= -13.7690 + 380.429d + 5197.48d^2 + (0.818816 + 3517.90d^2)\ln d \\
C_3(d) &= 35.0883 - 1079.70d - 14530.3d^2 - (1.44344 + 9855.73d^2)\ln d \\
C_4(d) &= -28.6643 + 927.876d + 12010.0d^2 + (0.571812 + 8221.82d^2)\ln d \\
&\qquad\qquad \text{for } 0.001 \le d \le 0.1
\end{aligned} \tag{11}$$

and

$$\begin{aligned}
C_1(d) &= -2.17381 - 11.3578d + 249.523d^2 - 729.371d^3 \\
&\quad + 489.172d^4 - (3.58885 - 74.3257d^2 + 335.732d^4)\ln d \\
C_2(d) &= 112.769 - 851.870d - 21390.1d^2 + 56909.8d^3 \\
&\quad - 34787.5d^4 + (41.8243 - 9944.26d^2 + 22067.0d^4)\ln d \\
C_3(d) &= -1680.23 + 24753.1d + 498848d^2 - 1314310d^3 \\
&\quad + 792477d^4 - (526.628 - 244353d^2 + 497280d^4)\ln d \\
C_4(d) &= 7043.32 - 142907d - 2883470d^2 + 7668650d^3 \\
&\quad - 4648720d^4 + (2177.01 - 1407520d^2 + 2937180d^4)\ln d \\
&\qquad\qquad \text{for } 0.1 < d < 1
\end{aligned} \tag{12}$$

using with the relation $d = 0.74 d_\mathrm{b}$.[25] We note that the application of Equation (9) with Equations (10)—(12) is limited to the following ranges of λL and λd: $\lambda L \ge 3.480$ for $0.001 \le \lambda d \le 0.1$ and $\lambda L \ge 90$ for $0.1 < \lambda d < 1$. We also note that the relation between d and d_b is proposed for the linear KP chain and is, strictly speaking, applicable for $0.01 \le d_\mathrm{b} \le 0.8$.[25] The behavior of the present MC data is consistent with the KP theory prediction, although the MC values for $\alpha/k_\mathrm{B}T \le 1$ are slightly larger than the corresponding theoretical values.

In Figure 1, it is seen that $\lambda^{3/2}M[\eta]_{\rm t.k.}/N_{\rm A}L^{3/2}$ deviates upward gradually and slightly with increasing λL, although such behavior is visible only for $\alpha/k_{\rm B}T = 0$ on this scale. Such a deviation may be recognized clearly by examining the behavior of $[\eta]_{\rm t.k.}/[\eta]_{\rm mix}$ as a function of λL.

Figure 2

Figure 2 shows double-logarithmic plots of $[\eta]_{\rm t.k.}/[\eta]_{\rm mix}$ against λL. The open circles represent the MC values calculated from the $M[\eta]/N_{\rm A}n^{3/2}l^3$ values given in Table 1, the various directions of the pips having the same meaning as those in Figure 1. The data points for various $\alpha/k_{\rm B}T$ seem to form a single composite curve, indicating that $[\eta]_{\rm t.k.}/[\eta]_{\rm mix}$ is a function only of λL, although $[\eta]_{\rm mix}$ and $[\eta]_{\rm t.k.}$ themselves depend not only on λL but also on $\lambda d_{\rm b}$. The ratio $[\eta]_{\rm t.k.}/[\eta]_{\rm mix}$ is almost equal to unity for $\lambda L \lesssim 10$ and then increases monotonically with increasing λL for $\lambda L \gtrsim 10$. This is due to the fact that the average chain dimension of the rings of the trivial knot is larger than that of the rings of the non-trivial knot (having the same λL) and the ratio of the number of configurations of the trivial knot included in a given mixed ensemble is almost equal to unity for $\lambda L \lesssim 10$ and it decreases monotonically to zero with increasing λL.[1] As mentioned in the INTRODUCTION, $[\eta]_{\rm t.k.}/[\eta]_{\rm mix}$ becomes proportional to $(\lambda L)^{0.3}$ in the random-coil limit ($\lambda L \to \infty$). However, the range $\lambda L \leq 10^3$ investigated is still far from the limit as in the case of $\langle S^2\rangle$ shown in Figure 4 of Ref 1.

Figure 3

Figure 3 shows double-logarithmic plots of $10^{-23}\Phi$ (in mol^{-1}) against λL. The symbols and dashed curves have the same meaning as those in Figure 1. The MC values are calculated from the defining equation 1, which may be rewritten in the following form

$$\Phi = N_{\rm A}\left(\frac{M[\eta]}{N_{\rm A}n^{3/2}l^3}\right)\left(\frac{nl^2}{6\langle S^2\rangle}\right)^{3/2}, \tag{13}$$

using with the MC values of $M[\eta]/N_{\rm A}n^{3/2}l^3$ and $\langle S^2\rangle/nl^2$ given in Table 1. The dashed and solid horizontal segments represent the asymptotic values for $\Phi_{\rm mix}$ and $\Phi_{\rm t.k.}$, respectively, in the limit of $\lambda L \to \infty$ described below.

For $1 \leq \alpha/k_{\rm B}T \leq 30$, $\Phi_{\rm mix}$ initially decreases and then increases after passing through a minimum with increasing λL in the range of λL examined. In the case of $\alpha/k_{\rm B}T = 100$, $\Phi_{\rm mix}$ decreases monotonically with increasing λL. For $\alpha/k_{\rm B}T \leq 0.3$, $\Phi_{\rm mix}$ decreases monotonically and approaches the random-coil limiting value given by[16,23,24]

$$\lim_{\lambda L \to \infty} \Phi_{\rm mix} = 5.234 \times 10^{23}\ {\rm mol}^{-1}\,, \tag{14}$$

as indicated by the dashed horizontal segment in Figure 3. The quantity Φ depends, of course, not only on λL but also on $\lambda d_{\rm b}$ and becomes larger with increasing $\lambda d_{\rm b}$ at constant λL.

It is seen from Figure 3 that $\Phi_{\rm t.k.}$ deviates downward gradually from $\Phi_{\rm mix}$ for $\alpha/k_{\rm B}T \leq 1$, while $\Phi_{\rm t.k}$ agrees almost completely with $\Phi_{\rm mix}$ for $\alpha/k_{\rm B}T \geq 3$. Before proceeding to further examination of the behavior of $\Phi_{\rm t.k.}$, it is necessary to estimate the asymptotic value of $\Phi_{\rm t.k.}$ in the limit of $\lambda L \to \infty$. For such a purpose, the MC values of $\Phi_{\rm t.k.}$ for $\alpha/k_{\rm B}T = 0$ are extrapolated to the limit of $n \to \infty$ ($\lambda L \to \infty$).

Figure 4

Figure 4 shows plots of $10^{-23}\Phi_{\rm t.k.}$ (in ${\rm mol}^{-1}$) against $n^{-1/2}$ for the discrete KP ring of $\alpha/k_{\rm B}T = 0$ and $n \geq 50$ with the MC data of $\Phi_{\rm t.k.}$ (for $d_{\rm b}/l = 1$) reproduced from Figure 3, which are represented by the closed circles. In the figure, the $\Phi_{\rm t.k.}$ values for $d_{\rm b}/l = 0.1$, 0.15, 0.2, 0.3, 0.4, and 0.5, which are evaluated in the same manner as in the case of $d_{\rm b}/l = 1$ (the details being omitted here), are also plotted. The dashed curves connect smoothly the data points for each $d_{\rm b}/l$ and the thin solid lines represent the initial tangents of the corresponding curves. The data for each $d_{\rm b}/l$ seem to converge to a constant independent of $d_{\rm b}/l$ in the limit of $n^{-1/2} \to 0$ ($n \to \infty$), and also, the data for $d_{\rm b}/l = 0.15$ have a good linearity in the range of small $n^{-1/2}$, which allows us a linear extrapolation to $n^{-1/2} = 0$. The asymptotic value of $\Phi_{\rm t.k.}$ may then be estimated as follows,

$$\lim_{\lambda L \to \infty} \Phi_{\rm t.k.} = 3._5 \times 10^{23}\ {\rm mol}^{-1}, \tag{15}$$

as indicated by the solid horizontal line segment in Figure 4 and also in Figure 3.

Figure 5

Figure 5 shows double-logarithmic plots of $\Phi_{\rm t.k.}/\Phi_{\rm mix}$ against λL. The symbols have the same meaning as those in Figure 2. The (thick) solid line segment represents the ratio 0.6_6 $[= 3._5 \times 10^{23}/(5.234 \times 10^{23})]$ of the asymptotic value of $\Phi_{\rm t.k.}$ given by Equation (15) to that of $\Phi_{\rm mix}$ given by Equation (14). The data points seem to form a single composite curve independent of $\lambda d_{\rm b}$ although $\Phi_{\rm t.k.}$ and $\Phi_{\rm mix}$ themselves depend on $\lambda d_{\rm b}$. The ratio $\Phi_{\rm t.k.}/\Phi_{\rm mix}$ is almost equal to unity for $\lambda L \lesssim 10$ and decreases monotonically with increasing λL. These results are consistent with those for $[\eta]_{\rm t.k.}/[\eta]_{\rm mix}$. The ratio $\Phi_{\rm t.k.}/\Phi_{\rm mix}$ is considered to become the constant 0.6_6 independent of λL in the limit of $\lambda L \to \infty$. Unfortunately, it is difficult to confirm such asymptotic behavior only on the basis of the present MC data for $\lambda L \leq 10^3$.

CONCLUSION

We have examined the effects of the chain stiffness and also the topological constraint on the intrinsic viscosity $[\eta]$ of semiflexible ring polymers by MC simulations using the discrete KP ring. It has been found that the ratio of $[\eta]$ for the rings of the trivial knot to that of the rings without the topological constraint becomes a function only of λL, which is almost equal to unity for $\lambda L \lesssim 10$ and increases monotonically with increasing λL for $\lambda L \gtrsim 10$, although $[\eta]$'s themselves depend not only on λL but also on $\lambda d_{\rm b}$.

(REFERENCES)

1 Ida, D., Nakatomi, D. & Yoshizaki, T. A Monte Carlo study of the second virial coefficient of semiflexible ring polymers. *Polym. J.* **42**, 735–744 (2010).

2 Tsubouchi, R., Ida, D., Yoshizaki, T. & Yamakawa, H. Scattering function of wormlike rings. *Macromolecules* **47**, 1449–1454 (2014).

3 Ida, D. Dilute solution properties of semiflexible star and ring polymers. *Polym. J.* **46**, 399–404 (2014).

4 Frank-Kamenetskii, M. D., Lukashin, A. V., Anshelevich, V. V. & Vologodskii, A. V. Torsional and bending rigidity of the double helix from data on small DNA rings. *J. Biomol. Struct. Dynam.* **2**, 1005–1012 (1985).

5 Kratky, O. & Porod, G. Röntgenuntersuchung gelöster fadenmoleküle. *Recl. Trav. Chim. Pay-Bas.* **68**, 1106–1122 (1949).

6 Yamakawa, H., *Helical Wormlike Chains in Polymer Solutions* (Springer, Berlin, 1997).

7 Kramers, H. A. The behavior of macromolecules in inhomogeneous flow. *J. Chem. Phys.* **14**, 415–424 (1946).

8 Zimm, B. H. & Stockmayer, W. H. The dimensions of chain molecules containing branches and rings. *J. Chem. Phys.* **17**, 1301–1314 (1949).

9 Yamakawa, H. *Modern Theory of Polymer Solutions* (Harper & Row, New York, 1971). Its electronic edition is available on-line at the URL: `http://www.molsci.polym.kyoto-u.ac.jp/archives/redbook.pdf`

10 des Cloizeaux, J. Ring polymers in solution: topological effects. *J. Phys. Lett.* **42**, L-433–L-436 (1981).

11 Grosberg, A. Y. Critical exponents for random knots. *Phys. Rev. Lett.* **85**, 3858–3861 (2000).

12 Takano, A., Kushida, Y., Ohta, Y., Matsuoka, K. & Matsushita, Y. The second virial coefficients of highly-purified ring polystyrenes. *Polymer* **50**, 1300–1303 (2009) and succeeding papers.

13 Terao, K., Asano, N., Kitamura, S. & Sato, T. Rigid cyclic polymer in solution: cycloamylose tris(phenylcarbamate) in 1,4-dioxane and 2-ethoxyethanol. *ACS Macro Lett.* **1**, 1291–1294 (2012) and succeeding papaers.

14 Kirkwood, J. G. & Riseman, J. The intrinsic viscosities and diffusion constants of flexible macromolecules in solution. *J. Chem. Phys.* **16**, 565–573 (1948).

15 Flory, P. J. & Fox Jr., T. G. Treatment of intrinsic viscosities. *J. Am. Chem. Soc.* **73**, 1904– 1908 (1951).

16 Fujii, M. & Yamakawa, H. Moments and transport coefficients of wormlike rings. *Macromolecules* **8**, 792–799 (1975).

17 Shimada, J. & Yamakawa, H. Moments for DNA topoisomers: The helical wormlike chain. *Biopolymers* **27**, 657–673 (1988).

18 Deutsch, J. M. Equilibrium size of large ring molecules. *Phys. Rev. E* **59**, R2539–R2541 (1999).

19 Metropolis, N., Rosenbluth, A. W., Rosenbluth, M. N., Teller, A. H. & Teller, E. Equation of state calculations by fast computing machines. *J. Chem. Phys.* **21**, 1087–1092 (1953).

20 Vologodskii, A. V., Lukashin, A. V., Frank-Kamenetskii, M. D. & Anshelevich, V. V. The knot problem in statistical mechanics of polymer chains. *Zh. Eksp. Teor. Fiz.* **66**, 2153–2163 (1974) [*Soviet Phys. JETP* **39**, 1059–1063 (1974)].

21 Crowell, R. H. & Fox, R. H., *Introduction to Knot Theory* (Ginn, Boston, 1963).

22 Matsumoto, M. & Nishimura, T. Mersenne Twister: A 623-dimensionally equidistributed uniform pseudo-random number generator. *ACM Trans. Model. Comput. Simul.* **8**,

3–30 (1998), see also the URL: http://www.math.sci.hiroshima-u.ac.jp/~m-mat/MT/emt.html

23 Bloomfield, V. A. & Zimm, B. H. Viscosity, sedimentation, et cetera, of ringand straightchain polymers in dilute solution. *J. Chem. Phys.* **44**, 315–323 (1966).

24 Fukatsu, M & Kurata, M. Hydrodynamic properties of flexiblering macromolecules. *J. Chem. Phys.* **44**, 4539–4545 (1966).

25 Yoshizaki, T., Nitta, I., & Yamakawa, H. Transport coefficients of helical wormlike chains. 4. Intrinsic viscosity of the touched-bead model. *Macromolecules* **21**, 165–171 (1988).

Table 1 Values of $M[\eta]/N_{\rm A}n^{3/2}l^3$ and $\langle S^2\rangle/nl^2$

n	$M[\eta]_{\rm mix}/N_{\rm A}n^{3/2}l^3$ (error %)	$\langle S^2\rangle_{\rm mix}/nl^2$ [a]	$M[\eta]_{\rm t.k.}/N_{\rm A}n^{3/2}l^3$ (error %)	$\langle S^2\rangle_{\rm t.k.}/nl^2$ [a]
		$\alpha/k_{\rm B}T = 0$		
10	0.779_4 (0.2)	0.0916_5	0.779_0 (0.2)	0.0921_1
20	0.662_1 (0.1)	0.0875_6	0.662_1 (0.1)	0.0886_5
50	0.558_4 (0.1)	0.0849_9	0.563_1 (0.1)	0.0878_6
100	0.501_9 (0.1)	0.0841_1	0.512_2 (0.0)	0.0891_5
200	0.458_2 (0.0)	0.0838_0	0.477_4 (0.1)	0.0921_9
500	0.413_8 (0.1)	0.0834_9	0.451_0 (0.1)	0.0982_6
1000	0.388_4 (0.1)	0.0833_6	0.445_7 (0.2)	0.105_0
		$\alpha/k_{\rm B}T = 0.3$		
10	0.754_0 (0.1)	0.115_0	0.753_0 (0.1)	0.115_2
20	0.719_6 (0.1)	0.116_2	0.720_1 (0.1)	0.117_1
50	0.678_1 (0.1)	0.116_9	0.683_3 (0.1)	0.119_7
100	0.650_8 (0.1)	0.117_3	0.663_0 (0.1)	0.122_7
200	0.624_9 (0.1)	0.117_3	0.649_4 (0.1)	0.126_6

(continued)

		$\alpha/k_{\rm B}T = 1$		
10	0.792_2 (0.0)	0.164_8	0.792_2 (0.1)	0.164_8
20	0.919_4 (0.1)	0.189_4	0.918_9 (0.1)	0.189_8
50	1.04_3 (0.1)	0.205_0	1.04_7 (0.1)	0.207_1
100	1.10_9 (0.1)	0.209_8	1.12_2 (0.2)	0.215_2
200	1.15_6 (0.1)	0.212_1	1.19_0 (0.1)	0.222_8
		$\alpha/k_{\rm B}T = 3$		
10	0.848_7 (0.0)	0.223_4	0.848_7 (0.1)	0.223_4
20	1.28_5 (0.2)	0.342_5	1.28_5 (0.1)	0.342_6
50	2.00_2 (0.4)	0.455_0	2.00_4 (0.3)	0.456_1
100	2.50_0 (0.2)	0.495_5	2.51_0 (0.3)	0.499_4
200	2.94_7 (0.2)	0.515_4	2.98_1 (0.1)	0.526_1
		$\alpha/k_{\rm B}T = 10$		
10	0.886_4 (0.0)	0.249_7	0.886_9 (0.1)	0.249_7
20	1.55_5 (0.1)	0.457_3	1.55_4 (0.0)	0.457_4
50	3.52_7 (0.1)	0.929_5	3.52_7 (0.1)	0.929_4
100	5.83_9 (0.2)	1.28_3	5.84_8 (0.2)	1.28_5

(continued)

200	8.34_6 (0.2)	1.49_0	8.34_1 (0.2)	1.49_3
		$\alpha/k_{\rm B}T = 30$		
10	0.898_7 (0.1)	0.257_7	0.899_1 (0.0)	0.257_7
20	1.64_4 (0.1)	0.492_4	1.64_5 (0.1)	0.492_4
50	4.24_6 (0.0)	1.15_2	4.24_6 (0.1)	1.15_2
100	8.83_1 (0.1)	2.07_3	8.83_1 (0.1)	2.07_3
200	16.8_5 (0.2)	3.25_2	16.8_6 (0.2)	3.25_3
		$\alpha/k_{\rm B}T = 100$		
10	0.903_4 (0.1)	0.260_6	0.903_4 (0.1)	0.260_6
20	1.67_8 (0.0)	0.505_2	1.67_8 (0.1)	0.505_2
50	4.51_9 (0.1)	1.23_3	4.51_8 (0.1)	1.23_3
100	10.0_9 (0.1)	2.39_2	10.1_0 (0.0)	2.39_2
200	22.7_1 (0.2)	4.50_3	22.7_1 (0.2)	4.50_3

[a] Reproduced from Table 2 of ref 1.

Figure Legends

Figure 1 Double-logarithmic plots of $\lambda^{3/2}M[\eta]/N_{\rm A}L^{3/2}$ against λL. The open and closed circles represents the MC values of $\lambda^{3/2}M[\eta]_{\rm mix}/N_{\rm A}L^{3/2}$ and $\lambda^{3/2}M[\eta]_{\rm t.k.}/N_{\rm A}L^{3/2}$, respectively, for $\alpha/k_{\rm B}T = 0$ (pip up), 0.3 (pip right-up), 1 (pip right), 3 (pip right-down), 10 (pip down), 30 (pip left-down), and 100 (pip left). The dashed curves connect smoothly the MC values of $\lambda^{3/2}M[\eta]_{\rm mix}/N_{\rm A}L^{3/2}$ for each $\alpha/k_{\rm B}T$. The solid horizontal line segment represents the random-coil limiting value[16,23,24] 0.3078 of $\lambda^{3/2}M[\eta]_{\rm mix}/N_{\rm A}L^{3/2}$. The solid curves represent the theoretical values for $\lambda^{3/2}M[\eta]_{\rm mix}/N_{\rm A}L^{3/2}$ of the KP cylinder ring[16] (see text).

Figure 2 Double-logarithmic plots of $[\eta]_{\rm t.k.}/[\eta]_{\rm mix}$ against λL. The closed circles represent the MC values with the various directions of the pips having the same meaning as those in Figure 1.

Figure 3 Double-logarithmic plots of $10^{-23}\Phi$ (in mol^{-1}) against λL. The open and closed circles represents the MC values of $\Phi_{\rm mix}$ and $\Phi_{\rm t.k.}$, respectively, with the various directions of the pips having the same meaning as those in Figure 1. The dashed curves connect smoothly the MC values of $\Phi_{\rm mix}$ for each $\alpha/k_{\rm B}T$. The dashed horizontal line segment represents the random-coil limiting value 5.234×10^{23} of $\Phi_{\rm mix}$[16,23,24] and the solid horizontal line segment represents the corresponding value $3._5 \times 10^{23}$ of $\Phi_{\rm t.k.}$ (see text).

Figure 4 Plots of $10^{-23}\Phi_{\rm t.k.}$ (in mol^{-1}) against $n^{-1/2}$ for the discrete KP ring of $\alpha/k_{\rm B}T = 0$ in the range of $n \geq 50$. The closed circles represents the MC values with indicated values of $d_{\rm b}/l$. The dashed curves connect smoothly the MC values for each $d_{\rm b}/l$ and the solid line segments represent the initial tangents of the corresponding curves. The (thick) solid horizontal line segment represents the random-coil limiting value $3._5 \times 10^{23}$ of $\Phi_{\rm t.k.}$ (see text).

Figure 5 Double-logarithmic plots of $\Phi_{\rm t.k.}/\Phi_{\rm mix}$ against λL. The closed circles represent

the MC values with the various directions of the pips having the same meaning as those in Figure 1. The solid horizontal line segment represents the ratio 0.6_6 of the random-coil limiting value of $\Phi_{\text{t.k.}}$ to that of Φ_{mix}.

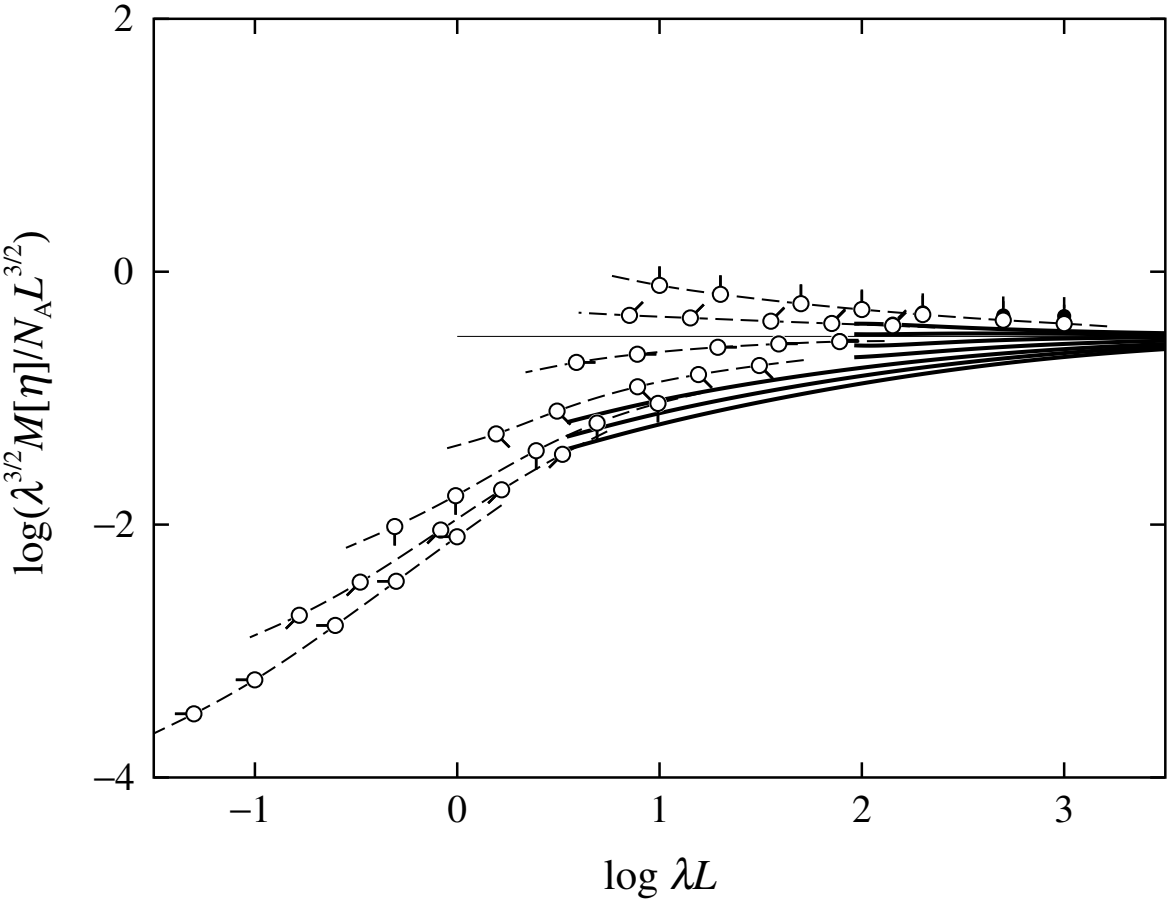

Y. Ono and D. Ida, Figure 1

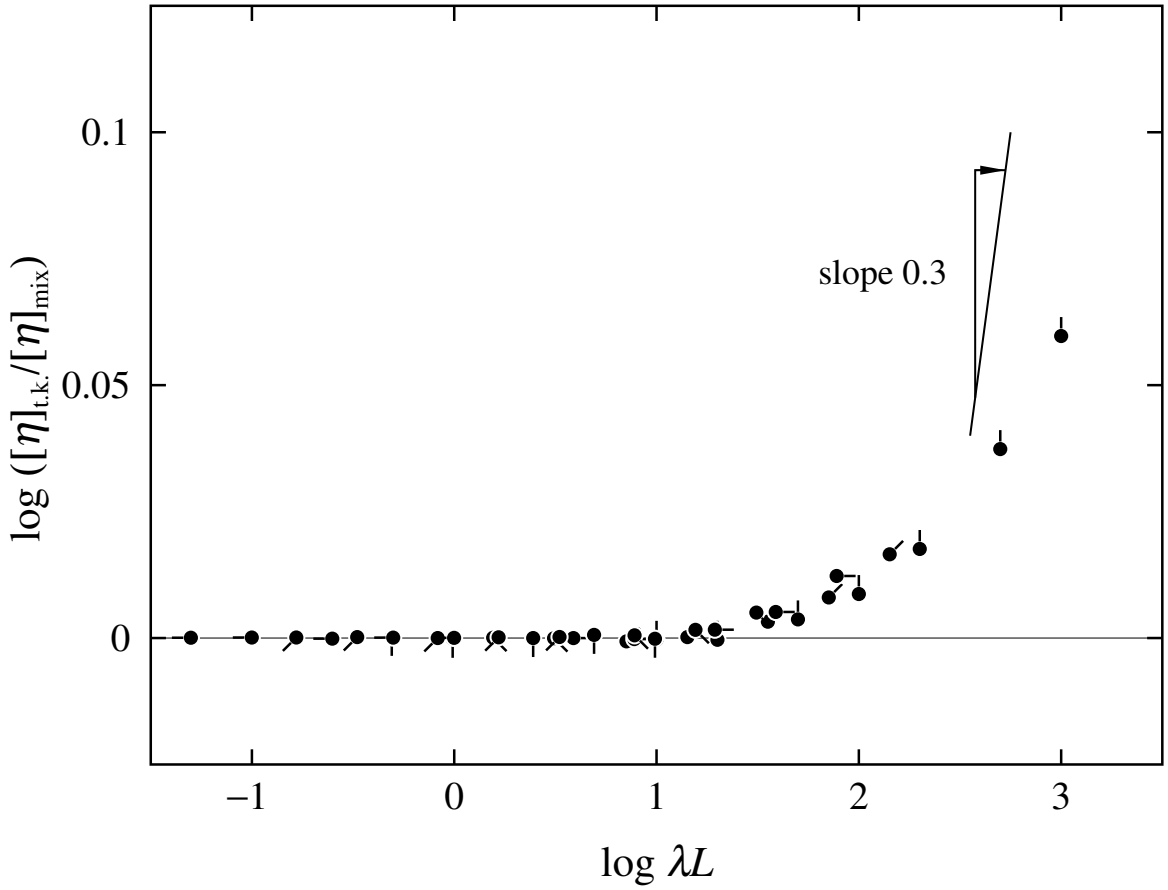

Y. Ono and D. Ida, Figure 2

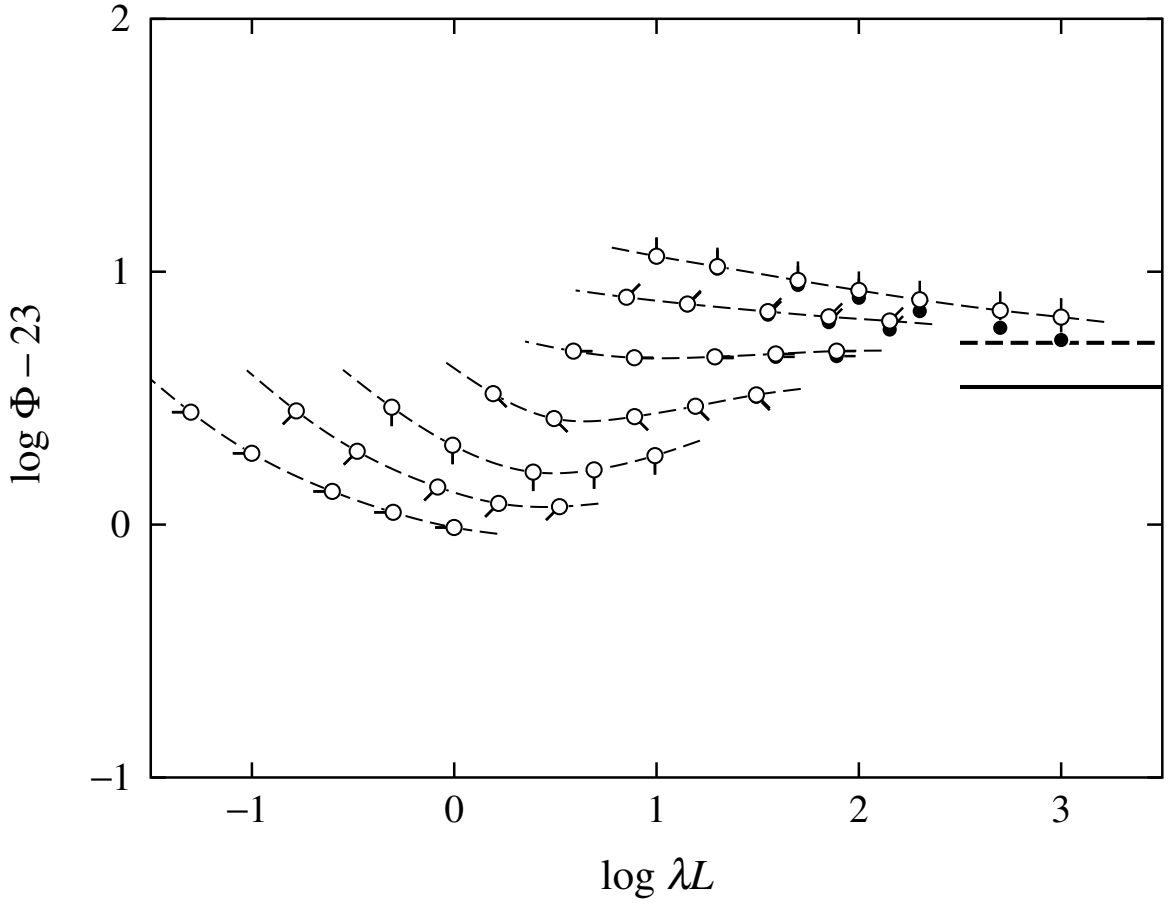

Y. Ono and D. Ida, Figure 3

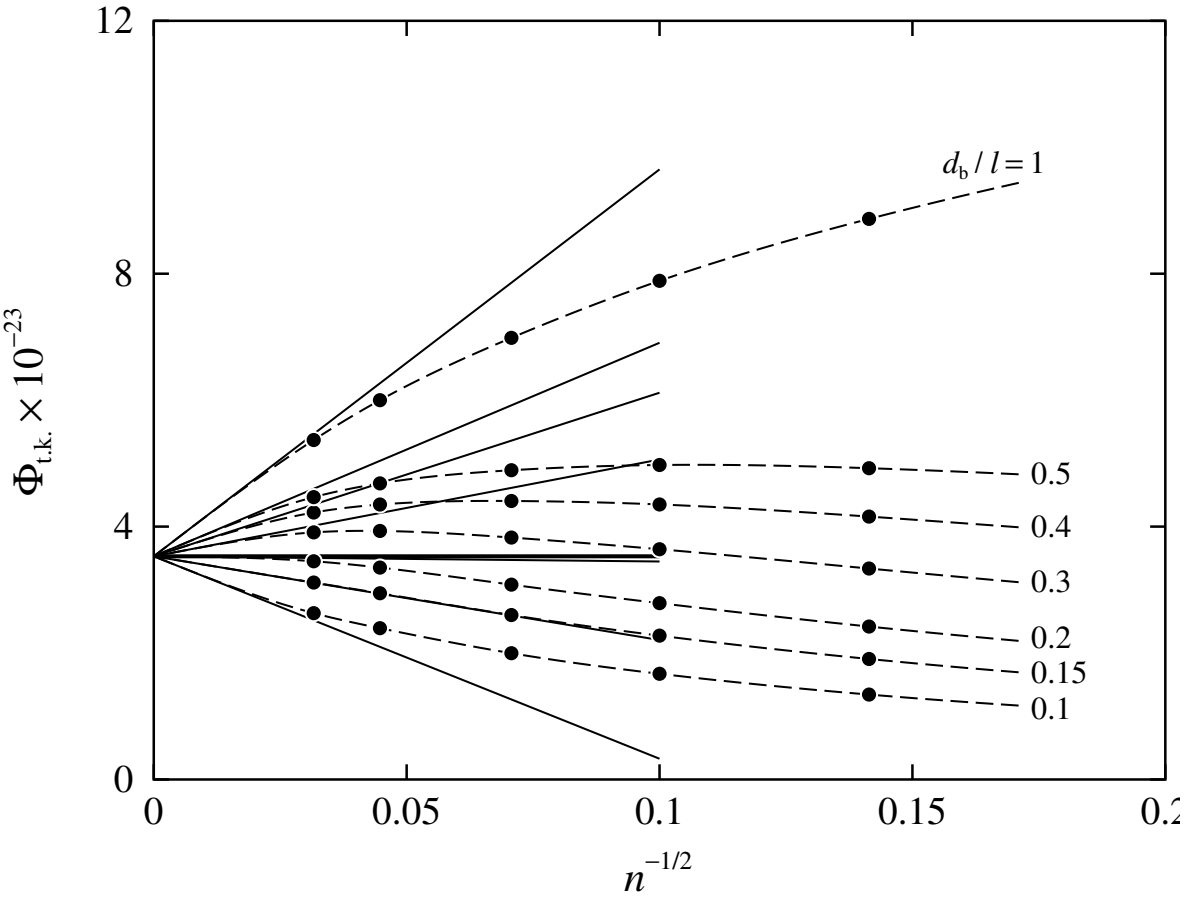

Y. Ono and D. Ida, Figure 4

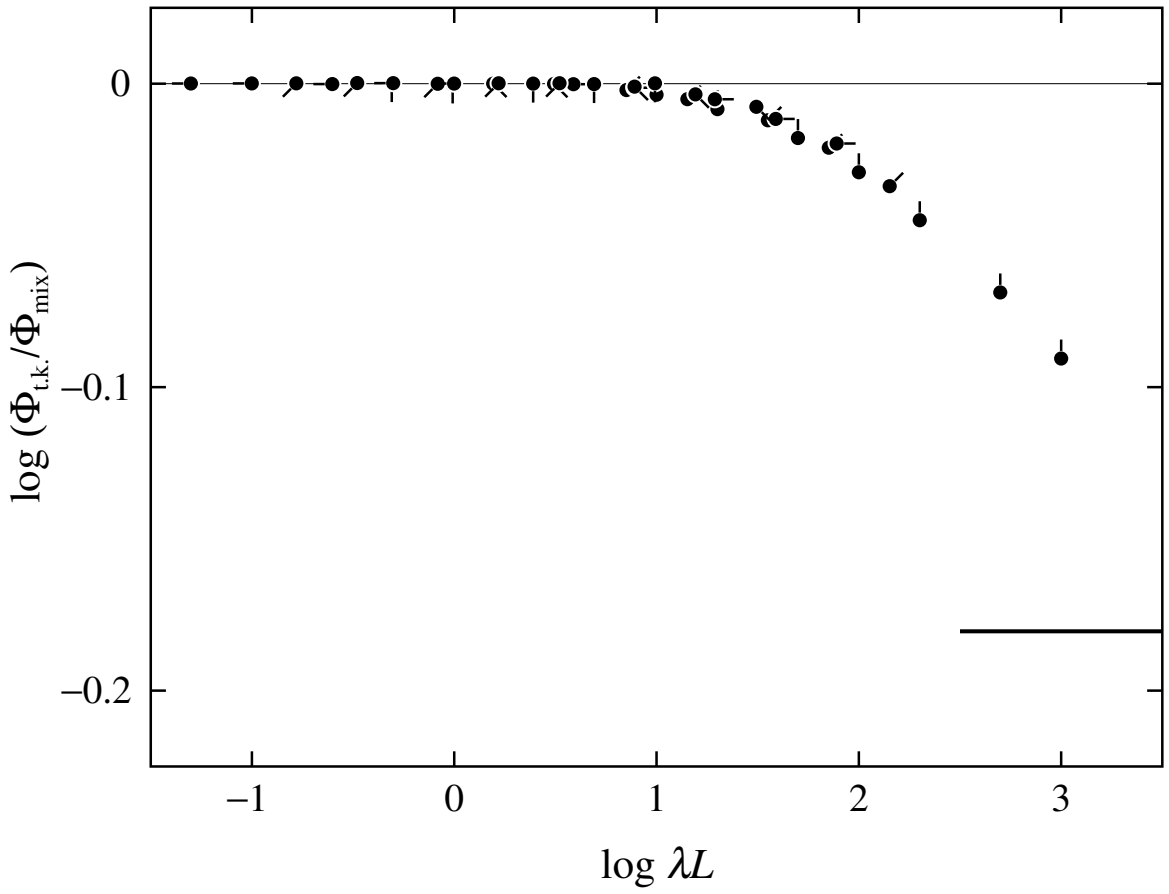

Y. Ono and D. Ida, Figure 5

Graphical Abstract:

The intrinsic viscosity $[\eta]$ of the Kratky–Porod (KP) wormlike rings is evaluated by Monte Carlo simulations. The behavior of the ratio of $[\eta]$ of the rings of the trivial knot ($[\eta]_{\mathrm{t.k.}}$) to that of the rings without the topological constraint ($[\eta]_{\mathrm{mix}}$) is examined as a function of the reduced contour length λL, where λ^{-1} is the stiffness parameter of the KP ring and L is the total contour length.